HHS Public Access

Author manuscript

Sci Transl Med. Author manuscript; available in PMC 2016 September 19.

Published in final edited form as:

Sci Transl Med. 2011 June 22; 3(88): 88ra54. doi:10.1126/scitranslmed.3002103.

Dosage Thresholds for AAV2 and AAV8 Photoreceptor Gene Therapy in Monkey

Luk H. Vandenberghe[1,*], **Peter Bell**[1], **Albert M. Maguire**[2,3], **Cassia N. Cearley**[4,5], **Ru Xiao**[1], **Roberto Calcedo**[1], **Lili Wang**[1], **Michael J. Castle**[4,5], **Alexandra C. Maguire**[2,†], **Rebecca Grant**[1], **John H. Wolfe**[4,5], **James M. Wilson**[1,‡], and **Jean Bennett**[2,3,‡]

[1]Gene Therapy Program, Department of Pathology and Laboratory Medicine, University of Pennsylvania, Philadelphia, PA 19104, USA.

[2]F. M. Kirby Center for Molecular Ophthalmology, Scheie Eye Institute, University of Pennsylvania, Philadelphia, PA 19104, USA.

[3]Center for Cellular and Molecular Therapeutics, Children's Hospital of Philadelphia, Philadelphia, PA 19104 USA.

[4]W. F. Goodman Center for Comparative Medical Genetics, School of Veterinary Medicine and Department of Pediatrics, School of Medicine, University of Pennsylvania, Philadelphia, PA 19104, USA.

[5]Stokes Research Institute, Children's Hospital of Philadelphia, Philadelphia, PA 19104, USA.

Abstract

Gene therapy is emerging as a therapeutic modality for treating disorders of the retina. Photoreceptor cells are the primary cell type affected in many inherited diseases of retinal degeneration. Successfully treating these diseases with gene therapy requires the identification of efficient and safe targeting vectors that can transduce photoreceptor cells. One serotype of adeno-associated virus, AAV2, has been used successfully in clinical trials to treat a form of congenital blindness that requires transduction of the supporting cells of the retina in the retinal pigment

‡To whom correspondence should be addressed. wilsonjm@mail.med.upenn.edu (J.M.W.); jebennet@mail.med.upenn.edu (J.B.).
*Present address: F. M. Kirby Center for Molecular Ophthalmology, Scheie Eye Institute, University of Pennsylvania, Philadelphia, PA 19104, USA.
†Present address: Princeton University, Princeton, NJ 08155, USA.

Author contributions: L.H.V., J.M.W., and J.B. designed the research approach. R.G., L.H.V., J.B., and J.M.W. obtained regulatory approvals. A.M.M. carried out the surgery with assistance from J.B., L.H.V., and R.G. R.G. provided veterinary oversight and obtained tissue samples. J.B. and A.M.M. carried out in vivo evaluations of GFP expression and performed fundus photography. L.W. and R.C. performed immunologic studies. P.B., L.H.V., R.X., J.M.W., and J.B. carried out ocular histologic evaluations. C.N.C., M.J.C., and J.H.W. performed lateral geniculate nuclei histology and the interpretation thereof. A.C.M. did visual behavior studies and video editing. L.H.V., J.M.W., and J.B. wrote the paper.

Competing interests: J.M.W. is a consultant to ReGenX Holdings and is a founder of, holds equity in, and receives a grant from affiliates of ReGenX Holdings. J.M.W. is an inventor on a patent licensed to various biopharmaceutical companies (adeno-associated virus serotype 8 sequences, vectors containing same, and uses thereof; USPTO 20080075740, WO/2003/052051). A.M.M. and J.B. are co-inventors on a pending patent for a method to treat or slow the development of blindness (WO/2002/082904, PCT/US2002/011314); both waived any financial interest in this technology in 2002. J.B. served on a scientific advisory board for Sanofi-Aventis and as a consultant for GlaxoSmithKline in 2010. The other authors declare that they have no competing interests.

Citation: L. H. Vandenberghe, P. Bell, A. M. Maguire, C. N. Cearley, R. Xiao, R. Calcedo, L. Wang, M. J. Castle, A. C. Maguire, R. Grant, J. H. Wolfe, J. M. Wilson, J. Bennett, Dosage thresholds for AAV2 and AAV8 photoreceptor gene therapy in monkey. *Sci. Transl. Med.* **3**, 88ra54 (2011).

epithelium (RPE). Here, we determined the dose required to achieve targeting of AAV2 and AAV8 vectors to photoreceptors in nonhuman primates. Transgene expression in animals injected subretinally with various doses of AAV2 or AAV8 vectors carrying a green fluorescent protein transgene was correlated with surgical, clinical, and immunological observations. Both AAV2 and AAV8 demonstrated efficient transduction of RPE, but AAV8 was markedly better at targeting photoreceptor cells. These preclinical results provide guidance for optimal vector and dose selection in future human gene therapy trials to treat retinal diseases caused by loss of photoreceptors.

INTRODUCTION

There is an unmet clinical need for approaches to treat both inherited monogenetic and complex retinal degenerative disorders in which the disease originates in photoreceptor cells of the retina. The eye is an attractive target organ for gene therapy because of its accessibility, small size, compartmentalized structure, well-defined blood-retina barrier, and its characteristic of being an immune-privileged site. Because of these features, a gene delivery agent can be administered in low doses and has limited systemic distribution. In recent successful Phase I and II clinical trials for a childhood-onset blindness called Leber congenital amaurosis, a recombinant adeno-associated virus serotype 2 (AAV2) targeting vector was used to deliver a therapeutic transgene to cells of the retinal pigment epithelium (RPE). In this form of Leber congenital amaurosis, mutations in the *RPE65* gene result in lack of production of a key enzyme in the vitamin A cycle, the side effects of which include the inability of rod photoreceptors to initiate the process leading to vision as well as toxicity to the RPE cells secondary to buildup of retinyl esters. RPE cell atrophy leads to secondary toxicity to photoreceptor cells, which are located above the RPE layer (1–3). Gene therapy could also be applied to diseases of retinal degeneration that are due to primary loss of photoreceptor cells such as most forms of retinitis pigmentosa (RP), a heterogeneous group of diseases with a wide spectrum of genotypes and phenotypes that affect up to 100,000 people in the United States. RP includes disease subsets such as congenital blindness (Leber congenital amaurosis), syndromes in which RP is a component (Usher syndrome, RP and deafness; Bardet-Biedl syndrome, polydactyly, mental retardation, and RP), and inherited macular degeneration (Stargardt disease) (4, 5). The feasibility of therapeutic gene delivery to treat these diseases will depend on the nature and degree of degeneration of the diseased retina as well as the capabilities and properties of the gene delivery vector. Tropism for the therapeutic target, appropriate amounts of transgene product, and restriction of therapeutic gene expression to the relevant cell types are factors that affect the safety and efficacy profile of any gene delivery tool (5).

The first AAV serotype considered as a vehicle for gene transfer was AAV2, which was developed from a cloned wild-type virus in the 1980s (6). One of the early applications of AAV2 was in settings of in vivo gene transfer in the eye. In the retina, outer retinal cells (photoreceptors and RPE cells) were transduced most efficiently after a subretinal route of injection (7–9), whereas inner retinal cells were transduced after injection into the vitreous humor (10, 11). These encouraging findings led to the exploration of other AAV serotypes for in vivo gene transfer (12). Many AAV serotypes have been described, and studies in the

retina have demonstrated that tropism, onset of transgene expression, and specificity of transduction can vary according to serotype and host species (13–15). Here, we compare AAV2 and AAV8 across a wide dose range in the cynomolgus macaque, an animal that, like humans, has a macula. This large-animal model also allowed the use of surgical maneuvers that are similar to those used in humans. Further, most large-animal studies describe the effects of exposure to doses higher than 1.5×10^{11} genome copies per eye, which to date is the maximum subretinal dose used in any of the AAV2 retinal gene therapy clinical trials (16). Studies in large animals with various AAV serotypes demonstrate consistent targeting of the RPE and, for most serotypes except AAV4, transduction of rod photoreceptor cells. Beltran *et al.* have highlighted the importance of the relationship of dose, gene transfer efficiency, and cellular specificity (17), which is not known for many AAV serotypes (18–21). There are conflicting reports on the ability of AAV2 to transduce cone photoreceptors (20, 22), but recent studies suggest that AAV5 at elevated doses can target cone photoreceptor cells (17, 23). The availability of vectors that can transduce rod and cone photoreceptors efficiently will expand the opportunities for treating or preventing blindness due to degeneration of these cells. AAV8 has emerged as a highly effective vector with broad tropism for many tissues and a favorable immunological profile (24–26).

Here, we selected AAV2 and AAV8 for qualitative and quantitative comparison of transgene expression in the monkey retina. In addition, the relationship of dose and variables related to subretinal delivery of AAV was studied using clinical examination, systemic indicators of inflammation, and extraocular neuronal expression. The use of a nonhuman primate model was important because cellular transduction details can differ depending on the species. Given that the eye of nonhuman primates is similar anatomically to the human eye and that these animals physiologically resemble humans in other characteristics such as immune response, this animal model is likely to be more predictive of the utility of these targeting vectors in humans.

RESULTS

Reporter gene expression after subretinal injection of AAV2 and AAV8 at different doses

Both eyes of 14 cynomolgus macaques were injected with either AAV2 or AAV8 expressing the enhanced green fluorescent protein (GFP) under control of the early cytomegalovirus promoter. The study design, specifics of injection, and clinical observations are summarized in Table 1. Briefly, both eyes were injected with the same virus serotype but at different doses: 10^8, 10^9, 10^{10}, and 10^{11} genome copies per eye for AAV8, and 10^{10} and 10^{11} genome copies per eye for AAV2. Other animal models have suggested that AAV8 has higher efficiency (13), and so to reduce animal use, we performed the AAV2 study after the AAV8 study in a dose de-escalating manner, and we terminated it at a dose of 10^{10} genome copies per eye because this dose yielded expression levels quantitatively comparable to that of AAV8. The subretinal injection was always in a similar site located on the superior temporal quadrant of the retina. In some cases, the AAV injection area extended through the fovea, the central point of the macula within the retina that contains exclusively cone photoreceptor cells (Table 1).

All animals tolerated the surgical delivery of AAV well, regardless of whether most of the material was retained under the retina or whether it leaked into the vitreal space. Leakage of blood into the subretinal space was observed during the intraoperative procedure in three of the eyes, and intraretinal blood was observed postoperatively in an additional eye (Table 1). Ocular media (fluid in the anterior and posterior segments within the eye) remained clear throughout the study, and no significant inflammatory reaction was observed at any time. Visual behavior testing after surgery confirmed that all of the animals had good visual acuity (videos S1 to S4 and Supplementary Results) even after administration of vector directly to the fovea (videos S1 and S2). However, the visual acuity of an animal that did not receive a foveal injection (animal 18180) was slightly less than that of the other animals. In four eyes (18144 right and left; 18199 right and 18208 right), retinal thinning in the center of the area correlating with the injection site was observed by ophthalmoscopy starting at 28 days after injection and was later confirmed by histology (see below).

After 7 days, the highest doses of AAV8 led to the earliest evidence of transgene expression by ophthalmoscopy (Table 1). All eyes injected with AAV2 at both doses showed GFP expression 21 days after injection, with increasing intensities through day 28 (Fig. 1). Two of the eyes showed reduced GFP expression thereafter (Table 1). The right eye of animal 18221 had received 10^{11} genome copies of AAV2 and showed moderate and broad expression in the superior temporal retina with increased focal GFP intensity in the fovea at days 21 and 28 (Fig. 1). However, from the second month after injection, expression was restricted to the fovea exclusively and disappeared entirely 4 months after injection (Table 1). GFP expression in the left eye of animal 18144 injected with 10^{10} genome copies of AAV2 was maximal after 1 month with a diffuse but broad pattern of transduction, but waned to a small GFP-positive area at month 3 with no visible GFP expression 4 months after injection (Table 1). Four months after injection, GFP expression from the 10^{8} genome copy dose of AAV8 was detectable in three of five eyes, whereas all other AAV8-injected eyes had detectable GFP expression before the end of the first month (Table 1 and Fig. 1).

After administration of 10^{10} and 10^{11} genome copies of AAV2 or AAV8, GFP expression was widespread but not always homogeneous. At 10^{10} and 10^{11} genome copy doses of either serotype, a circular rim of bright GFP expression enclosing an area of dim or hardly visible GFP signal (“halo”) was observed in a few eyes (Figs. 1 and 2A). Thus, comparison studies revealed a slightly earlier onset of GFP expression after delivery of AAV8 compared to AAV2 and similar patterns of GFP distribution, although GFP concentrations appeared higher dose for dose with AAV8 than with AAV2.

Retinal cell tropism and AAV serotype

At the lower doses of both targeting vectors (10^{10} genome copies for AAV2 and 10^{8} and 10^{9} genome copies for AAV8), the primary target was the RPE. Higher doses targeted greater numbers and a wider variety of cells in the neuronal retina, particularly photoreceptor cells (Fig. 3, A and B). As illustrated in Fig. 3A, 10^{11} genome copies of AAV2 and 10^{10} and 10^{11} genome copies of AAV8 resulted in widespread and bright GFP expression in photoreceptor cells and the RPE. Notably, at these doses, several regions of GFP-positive photoreceptor cells were identified that lacked GFP in the adjacent RPE. In these areas, regardless of GFP

positivity, the RPE and photoreceptors appeared healthy and viable as determined by 4′,6-diamidino-2-phenylindole (DAPI) staining.

Transduction of photoreceptor cells with AAV2 and AAV8 was essentially relegated to rod photoreceptors as judged by the well-defined shape and retinal locations of those cells. In the periphery of the retina, peanut agglutinin and cone arrestin immunofluorescence, used to stain cone photoreceptors, identified only limited GFP expression in this cell type, in terms of both the number of positive cells and the intensity of expression (fig. S1). The one notable exception was foveal photoreceptors, which consist entirely of cones. In the fovea, transduction was observed for AAV8 at 10^{10} genome copies but not for AAV2 (Fig. 3C). In monkey retinas where the fovea was exposed to vector, AAV8 transduced up to 30% of foveal cones at the 10^{10} genome copy dose; AAV2 achieved similar targeting but only at the 10^{11} genome copy dose. Neither vector demonstrated prominent cone transduction in the perifoveal regions, highlighting the overall low permissiveness of cones compared to rods for vector transduction even at this elevated dose (fig. S1). Müller cells, glial cells embedded in and critical for the sustenance of the neuronal retina, were also frequent targets of AAV2 and AAV8 transduction (Fig. 2D), with qualitatively more of those cells transduced with AAV8 than with AAV2 at the same doses.

Through correlative analysis of retinal imaging and histological data, we reconstructed the entire cross section of the transduced areas of each retina, including the regional differences noted by ophthalmoscopic observation (such as the halo patterns of transduction described above). These analyses illustrate GFP-positive photoreceptor cells throughout the vector-exposed area and that the halo patterns correspond to small portions of the RPE expressing GFP as shown in Fig. 2A for an eye injected with 10^{11} genome copies of AAV2 (animal 18226, right eye). In areas that showed histopathology (see below), there was reduced GFP expression noted both ophthalmoscopically and by microscopy. Within monkey retinas in which subretinal blood had been noted during the injection procedure, weidentified areasthat totallylacked GFP expression but were exposed to vector (Fig. 2, B and C). Those areas were also evaluated histopathologically in more detail (see below). Thus, both AAV2 and AAV8 transduce RPE efficiently at lower doses. At higher doses, AAV8 is more efficient than AAV2 at transducing photoreceptor cells. Targeting is largely restricted to rod photoreceptors; however, less efficient transduction of cone photoreceptors does occur particularly in the fovea at the highest doses.

Quantitative assessment of transduction

To quantitatively assess the relationship between vector dose and serotype and retinal transduction efficiency, we measured total retinal fluorescence and performed detailed morphometric analyses on histological sections. Eyes with noted injection problems such as intravitreal leakage or retinal bleed were excluded from these analyses (Table 1). Using postmortem whole retinal imaging, we detected GFP expression for all eyes injected with AAV8 at the two highest doses but not for the two lowest AAV8 doses. GFP expression was detected in only one of the 10^{10} genome copy and two of the 10^{11} genome copy AAV2-dosed eyes (Fig. 4, A and B). For the 10^{10} genome copy dose, AAV8 resulted consistently in

higher GFP expression than did AAV2. AAV2 can deliver similar transgene expression levels as AAV8, but it requires a 10-fold higher dose to do so.

Next, transduction intensity (Fig. 4C) and efficiency (Fig. 4D) in photoreceptors and RPE within the vector-exposed area of the retina were quantified per vector dose and serotype by morphometry of the fluorescent signal in the micrographs. Analyses were restricted to eyes that had received the entire vector dose subretinally in the absence of injection problems as noted in Table 1. Only 10^9 and 10^{10} genome copy dose groups were analyzed quantitatively because of the marginal signal at the lowest dose and the incidence of toxicity at the highest dose, which complicated quantification. AAV8 transduction in both photoreceptor and RPE cells is equally intense at the 10^{10} genome copy dose, whereas at 10^9 genome copies the GFP signal in photoreceptors is markedly reduced. The AAV2 transduction profile at 10^{10} genome copies is similar to that of AAV8 at a 10-fold lower dose.

Within the vector-exposed subretinal space, the 10^{10} genome copy dose of AAV2 and AAV8 targets 30 and 70%, respectively, of RPE and photoreceptor cells (Fig. 4D). AAV2 transduces photoreceptors at this dose, albeit at a much lower relative intensity compared to AAV8 (Fig. 4, C and D). Fifty percent of the RPE cells and 20% of photoreceptor cells are transduced with a 10^9 genome copy dose of AAV8. In the RPE, the relationship of AAV8 dose to transduction efficiency is nonlinear; a 10-fold higher dose realizes only a limited increase in GFP expression (Fig. 4, C and D). In contrast, a dose-related increase in photoreceptor transduction is apparent.

In summary, both AAV2 and AAV8 target the RPE efficiently at low doses. Substantial photoreceptor transduction is achieved at higher doses starting at 10^9 genome copies for AAV8 and at a 10-fold higher dose for AAV2.

Immune responses to GFP and the AAV capsid

Humoral and cellular immune responses to the capsid of the viral vector may affect the success of gene transfer. We therefore monitored several parameters of the host immune response to subretinal administration of AAV2 and AAV8 delivering GFP. Neutralizing antibody responses to the vector capsid were evaluated in anterior chamber fluid as well as in peripheral blood at time points before and after vector administration and at the time of necropsy. All animals in the study were negative for AAV-neutralizing antibodies at enrollment to minimize the impact of preexisting immunity on gene transfer. The host immune data are summarized in Table 2 and demonstrate a dose-related increase in neutralizing antibodies that is more pronounced in the serum than in the anterior chamber of the eye. With the exception of one eye dosed with 10^{10} genome copies of AAV2, only eyes injected with the highest dose of the vector had detectable levels of neutralizing antibodies in the anterior chamber fluid. In serum, at a dose of 10^{10} genome copies, two of five animals had a titer of 1:80, whereas seven of nine animals that received 10^{11} genome copies had titers of 1:80 to 1:640. There was no obvious correlation between eyes that developed anti-AAV–neutralizing antibodies in the anterior chamber fluid and increased intravitreal exposure to AAV (Table 1) or the presence of blood in the eye. Similarly, there was no obvious correlation between animals that showed increased anti-AAV–neutralizing antibodies in serum and increased intravitreal exposure to AAV. One animal (18226) that

developed high anti-AAV–neutralizing antibodies did have blood exposure in one eye (Table 1), but two others (18180 and 18208) did not.

Cellular immune responses to both the GFP transgene product and the vector capsid were assessed by the enzyme-linked immunospot (ELISPOT) assay and intracellular cytokine staining for interferon-γ in peripheral blood mononuclear cells at day 14 after injection and in leukocytes from blood, liver, and spleen at the time of necropsy. Before AAV injection, 9 of 14 animals demonstrated detectable T cell activation in response to the AAV capsid upon amplification in the cultured ELISPOT assay, an indication of memory T cell responses. However, all animals were negative in the ex vivo assay (Table 2). Before this study, animals had not been exposed to GFP antigen. After vector administration, ex vivo ELISPOT data from peripheral blood mononuclear cells demonstrated no evidence of T cell activation in response to vector capsid either at 2 weeks after vector administration or at necropsy. Animal 18144 that received 10^{10} and 10^{11} genome copies per eye of AAV2 presented with T cell reactivity to GFP at necropsy in the spleen and peripheral blood mononuclear cells. T cell activation in response to the GFP transgene product was also detected in the blood, liver, and spleen of an animal (18199) given a high dose of AAV8 vector. Thus, retinal delivery of high doses of AAV2 or AAV8 carrying GFP can lead to increases in anti-AAV–neutralizing antibodies locally and systemically and can also lead to a systemic T cell response to GFP.

Histopathology after subretinal injection of AAV2 and AAV8

Serial sections were taken throughout the area of the original retinal detachment where the AAV vectors were delivered. All sections were analyzed by DAPI staining of nuclei to evaluate retinal architecture. Hematoxylin and eosin (H&E) staining and immunohistochemistry were performed in areas where architecture was disrupted. Table 2 summarizes the results. Both retinas in the AAV2-injected animal 18144 showed retinal thinning in large portions of the exposed retina (Fig. 2B) due to loss of photoreceptor cells. Histopathology also showed foci of inflammatory cells within the retina and choroid (Fig. 2D). Pathological changes were also observed in animals 18199 and 18208 but were restricted to the right eye (Fig. 2, C and E), which received the highest dose (10^{11} genome copies) of vector. Here, too, foci of inflammatory cells, retinal thinning, and loss of the layered retinal structure in AAV-exposed regions were observed. Toxicity correlated with increased numbers of T cells in response to GFP in the periphery for animals 18144 and 18199, whereas no systemic inflammation was detected in animal 18208 (Table 2). Thus, exposure of the retina to high doses of AAV2 or AAV8 and/or high levels of GFP can lead to inflammatory changes that damage the retina.

AAV2 and AAV8 transduction of the optic pathway

Histological analysis for positive staining for GFP along the visual pathway leading from the ganglion cells in the retina to the central nervous system (optic nerve, optic chiasm, and the lateral geniculate nuclei) was evaluated directly by fluorescence microscopy. Transduction of the optic disc was apparent in all eyes injected with 10^{11} genome copies, irrespective of vector serotype or the extent to which the vitreous humor was exposed to vector, and in one eye injected with 10^{10} genome copies of AAV8 (Table 2). GFP was also detected in the optic chiasm and both the ipsilateral and the contralateral lateral geniculate nucleus for all animals

in the highest-dose cohort, irrespective of vector serotype. Exceptions were animals 18144 and 18199, which showed a T cell response to GFP (Table 2). Overall, there appeared to be more GFP-positive axons in animals injected with the higher doses of AAV8 compared to animals injected with the same doses of AAV2. No neuronal cell bodies in the lateral geniculate nuclei appeared to be positive for GFP, and there was no GFP detectable in the visual cortex (which is postsynaptic to the lateral geniculate nuclei). For each serotype, sections of the lateral geniculate nuclei from the animals with the greatest GFP expression in the lateral geniculate nuclei were stained with neutral red to visualize the layered structure of this region. Overlays of GFP staining and staining of cell organelles with neutral red stain are shown in fig. S2. The location of GFP-positive axons within the lateral geniculate nuclei directly correlated with known retinal projections and the retinal topography of the injection site in that the regions of the lateral genic ulate nuclei with the most GFP expression in axons were the regions receiving retinal projections from the eye injected with the highest titer of AAV8 or AAV2. The greatest number of GFP-positive axons was found in layer 2 of the right lateral geniculate nuclei and layer 1 of the left lateral geniculate nuclei. These layers receive inputs from the right eye, which received the highest titer of AAV8 or AAV2. GFP-positive axons were not observed in layers 3, 4, 5, or 6 of the lateral geniculate nuclei. Thus, retinal exposure to high doses of AAV2 or AAV8 can lead to transduction of a specific class of retinal ganglion cells.

DISCUSSION

Recent results from three concurrent Phase I clinical trials for the treatment of Leber congenital amaurosis type II showed the potential for gene therapies based on subretinally delivered AAV for treating other retinal degeneration disorders (27). Broader clinical application of AAV technology will require an expanded vector toolkit along with a deeper understanding of the pharmacological, immunological, and toxicological effects of vectors and other safety aspects. For Leber congenital amaurosis, reconstitution of the RPE65 protein in the RPE was necessary and sufficient to restore retinal function. Other therapeutic approaches will require more efficient gene transfer into other cell types, particularly photoreceptor cells. There is also a need for new technologies to be investigated in animal models that more closely resemble humans with respect to anatomy, size, and host immune response. To this end, nonhuman primates are a unique and necessary resource because only primates (including humans) have both a macula and a fovea. Host immune responses to the viral vector and transgene are thought to be similar in nonhuman primates and humans because both populations are genetically heterogeneous and AAV is endemic in both (25). Here, AAV2 and AAV8 viral vectors expressing a GFP reporter trans-gene under control of the cytomegalovirus promoter were injected subretinally in nonhuman primates. Vector transduction of photoreceptor cells and the host immune response were evaluated as a function of vector type and dose.

The data show that the RPE is exceptionally permissive for uptake of both AAV2 and AAV8 vectors. Although it is unclear how AAV2 performs at lower doses, the relative efficiency of RPE transduction by AAV8 at 10^9 genome copies is similar to that of AAV2 at a 10-fold higher dose. RPE transduction does not increase linearly at higher doses, and heterogeneous patterns of GFP expression are seen in the fundus, indicating a loss of GFP transgene

expression in an otherwise healthy RPE. Although these findings remain unexplained and have not been described previously in the retina, they could be attributable to RPE-specific epigenetic changes affecting the cytomegalovirus promoter leading to silencing of transgene expression (28).

Many retinal degeneration disorders affect cell types other than the RPE. Photoreceptor cells, the primary cell type involved in most retinal diseases, are a difficult cellular target for gene therapy, although progress has been made in mouse (13–15, 29), dog (17, 19, 21), and primate (20, 21) using improved vectors. Here, the relative efficiency of photoreceptor cell transduction by AAV2 and AAV8 was evaluated as a function of dose. AAV2 is less efficient compared to AAV8 at targeting photoreceptors with an ~10-fold dose differential. AAV8, at a dose of 10^{10} genome copies, transduces most rod photoreceptors but not cone photoreceptors within the vector-exposed area. Cones are poorly transduced, particularly in extrafoveal areas. In the fovea, targeting of cones is more efficient with AAV8 but can be achieved with AAV2 by increasing the vector dose. Previously, AAV5-mediated transduction was shown by Mancuso *et al.* to enhance color perception in a primate model of red-green color blindness (23, 30), which was presumed to result from cone-specific expression of the transgene. Lotery *et al.* (31) did not observe AAV5-mediated cone transduction in nonhuman primates, whereas Beltran *et al.* (17) did see this in dogs. The different conclusions of these studies may be attributable to differences in vector dose and promoter. An alternative explanation for the Mancuso *et al.* results is that rod photoreceptors were induced to behave like cones (because of transfer of L-opsin); such a possibility could be evaluated using an immunohistochemical label that is independent of the transgene. An AAV5 dosing study in nonhuman primates would also be helpful for evaluating the relative cone targeting efficiency of AAV5 compared to AAV2 or AAV8.

One vector-related concern is the extraocular distribution of the vector and transgene. The lateral geniculate nuclei carry visual information to the cerebral cortex and are the sites of the first synapse for 90% of axons coming from retinal ganglion cells. We and others have described transduction of retinal ganglion cells after intraocular administration of AAV (10, 11). Thus, it was not surprising in our new study to find GFP-positive axons that synapse with the lateral geniculate nuclei after delivery of the highest vector dose. However, unexpectedly, all of the synapses were in the lateral geniculate nuclei layers 1 and 2. These layers contain projections from M-type retinal ganglion cells, which are a minority (5 to 10%) of the ganglion cells in the retina (32). AAV2 and AAV8 may have a specific tropism for M-type retinal ganglion cells. Alternatively, M-type ganglion cells may be more accessible to vector leaking into the vitreous humor because they cover a large area of the retina owing to their extensively branched dendrites. It is less likely that vector diffuses from the subretinal space through the neuronal retina given the tight junctions between the cells. A third point of access may be the injection site in the peripheral macula, an area with denser M-type cells. Regardless of the route, it is clear that transduction of M-cells is favored and occurs efficiently at higher doses of AAV vectors. We did not observe transduction after the first synapse, which is similar to results reported in mice and dogs injected with AAV (10, 11) but different from studies in dogs using AAV8 (18). Nevertheless, these data support the use of cell-specific promoters for restricting transgene expression to primary outer retinal cellular targets.

Another safety aspect for AAV gene therapy targeting tissues including the eye is the immunological response to the AAV capsid and the transgene product. Several ocular compartments are immune-privileged based on their ability to accept foreign tissue grafts (33). But immune privilege could be breached through delivery of AAV and a foreign transgene. Immune responses and inherent toxicity to GFP could potentially contribute to the host immune response, although GFP was tolerated in previous studies in the nonhuman primate eye (20, 21). Here, intraocular administration of AAV2 and AAV8 led to increases in neutralizing antibodies to the vector capsid in a dose-related fashion. Potentially destructive T cell responses to the AAV capsid were not identified. However, evidence for responses to the GFP transgene product was found in two animals that had received the highest AAV dose. These particular animals demonstrated focal spots of retinal inflammation, retinal thinning, and disrupted retinal architecture (Table 2 and Fig. 2, B to E). For a few eyes, retinal bleeding was observed during the surgical delivery of vector. In one eye, which received the highest vector dose, inflammation was associated with leakage of blood under the retina. Retinal degeneration is a well-known consequence of exposure of photoreceptors to blood components (34, 35). Fortunately, toxicity has not been observed in AAV-treated Leber congenital amaurosis patients, even though similar vector doses were injected into these patients. Several factors may contribute to the dissimilar findings including differences between the animal model and clinical settings in terms of vector quality and surgical procedures. The use of a reporter transgene product, GFP, which is foreign to the host, is different from the clinical setting. For example, in the AAV–Leber congenital amaurosis clinical trials, patients were injected with an AAV vector carrying a human *RPE65* complementary DNA (cDNA). The studies in this report may reflect a worst-case scenario in which a transgene product is foreign to the host, as would be the case in gene addition strategies to correct *null* mutations.

Our studies describe the dose relationship between AAV2 and AAV8 vectors and immunotoxicity in the nonhuman primate retina. Although the monkeys in this study weigh only 5 to 10% of an average human, the axial length of the eye is comparable (~70% of the axial length of the human eye). This, together with the high degree of anatomical similarity, makes nonhuman primates a relevant model for evaluating vector dosing for clinical translation of retinal gene therapies. Our data indicate the existence of dosage thresholds that need to be met to safely and efficiently target cells in the outer retina such as RPE cells and rod and cone photoreceptors. Whereas AAV2 and AAV8 efficiently transduce RPE at moderate to low doses, AAV-mediated expression of a foreign transgene in rod and cone photoreceptors was reached only at higher dosages. Substantial transduction of rods was obtained with moderate doses of AAV8 (doses that are similar to those currently used in experimental clinical protocols; http://www.clinicaltrials.gov). Targeting cones with AAV2 or AAV8 is less efficient than rod transduction but can be achieved at higher doses. However, at higher doses, some animals in both vector groups showed histopathological evidence of inflammatory foci and retinal degeneration. This pathology is likely attributable to transgene-specific immune responses and a transient breach of the retina-blood barrier, resulting in exposure of vector and retina to blood products. Our data suggest that AAV8, because of its ability to efficiently and safely target both RPE and photoreceptors at

moderate doses, is an attractive gene transfer vehicle for gene therapy targeting the retina in patients with retinal degenerative diseases.

Supplementary Material

Refer to Web version on PubMed Central for supplementary material.

Acknowledgments

We thank T. Cronin and P. Sulaiman for assistance with confocal microscopy, P. Macleish (Morehouse School of Medicine, Atlanta, GA) for the 7G6 cone arrestin antibody, and T. Irvin and E. Bote for support with the animal work. **Funding:** Supported by grants to J.M.W. from GlaxoSmithKline Pharmaceuticals Inc.; to J.B. from Research to Prevent Blindness, Foundation Fighting Blindness, the Paul and Evanina Mackall Foundation Trust, and the F. M. Kirby Foundation; to J.H.W. from the National Institute of Neurological Disorders and Stroke (NS038690) and training support for C.N.C. (NS007180) and M.J.C. (NS007413); and to L.H.V. by grant UL1RR024134 from the National Center for Research Resources and the Institute for Translational Medicine and Therapeutics at the University of

REFERENCES AND NOTES

1. Bainbridge JW, Smith AJ, Barker SS, Robbie S, Henderson R, Balaggan K, Viswanathan A, Holder GE, Stockman A, Tyler N, Petersen-Jones S, Bhattacharya SS, Thrasher AJ, Fitzke FW, Carter BJ, Rubin GS, Moore AT, Ali RR. Effect of gene therapy on visual function in Leber's congenital amaurosis. N. Engl. J. Med. 2008; 358:2231–2239. [PubMed: 18441371]
2. Hauswirth WW, Aleman TS, Kaushal S, Cideciyan AV, Schwartz SB, Wang L, Conlon TJ, Boye SL, Flotte TR, Byrne BJ, Jacobson SG. Treatment of Leber congenital amaurosis due to RPE65 mutations by ocular subretinal injection of adeno-associated virus gene vector: Short-term results of a phase I trial. Hum. Gene Ther. 2008; 19:979–990. [PubMed: 18774912]
3. Maguire AM, Simonelli F, Pierce EA, Pugh EN Jr. Mingozzi F, Bennicelli J, Banfi S, Marshall KA, Testa F, Surace EM, Rossi S, Lyubarsky A, Arruda VR, Konkle B, Stone E, Sun J, Jacobs J, Dell'Osso L, Hertle R, Ma JX, Redmond TM, Zhu X, Hauck B, Zelenaia O, Shindler KS, Maguire MG, Wright JF, Volpe NJ, McDonnell JW, Auricchio A, High KA, Bennett J. Safety and efficacy of gene transfer for Leber's congenital amaurosis. N. Engl. J. Med. 2008; 358:2240–2248. [PubMed: 18441370]
4. Berger W, Kloeckener-Gruissem B, Neidhardt J. The molecular basis of human retinal and vitreoretinal diseases. Prog. Retin. Eye Res. 2010; 29:335–375. [PubMed: 20362068]
5. Surace EM, Auricchio A. Versatility of AAV vectors for retinal gene transfer. Vision Res. 2008; 48:353–359. [PubMed: 17923143]
6. Samulski RJ, Berns KI, Tan M, Muzyczka N. Cloning of adeno-associated virus into pBR322: Rescue of intact virus from the recombinant plasmid in human cells. Proc. Natl. Acad. Sci. U.S.A. 1982; 79:2077–2081. [PubMed: 6281795]
7. Ali RR, Reichel MB, Thrasher AJ, Levinsky RJ, Kinnon C, Kanuga N, Hunt DM, Bhattacharya SS. Gene transfer into the mouse retina mediated by an adeno-associated viral vector. Hum. Mol. Genet. 1996; 5:591–594. [PubMed: 8733124]
8. Bennett J, Duan D, Engelhardt JF, Maguire AM. Real-time, noninvasive in vivo assessment of adeno-associated virus-mediated retinal transduction. Invest. Ophthalmol. Vis. Sci. 1997; 38:2857–2863. [PubMed: 9418740]
9. Flannery JG, Zolotukhin S, Vaquero MI, LaVail MM, Muzyczka N, Hauswirth WW. Efficient photoreceptor-targeted gene expression in vivo by recombinant adeno-associated virus. Proc. Natl. Acad. Sci. U.S.A. 1997; 94:6916–6921. [PubMed: 9192666]
10. Dudus L, Anand V, Acland GM, Chen SJ, Wilson JM, Fisher KJ, Maguire AM, Bennett J. Persistent transgene product in retina, optic nerve and brain after intraocular injection of rAAV. Vision Res. 1999; 39:2545–2553. [PubMed: 10396623]

11. Guy J, Qi X, Muzyczka N, Hauswirth WW. Reporter expression persists 1 year after adeno-associated virus-mediated gene transfer to the optic nerve. Arch. Ophthalmol. 1999; 117:929–937. [PubMed: 10408459]
12. Vandenberghe LH, Wilson JM, Gao G. Tailoring the AAV vector capsid for gene therapy. Gene Ther. 2009; 16:311–319. [PubMed: 19052631]
13. Allocca M, Mussolino C, Garcia-Hoyos M, Sanges D, Iodice C, Petrillo M, Vandenberghe LH, Wilson JM, Marigo V, Surace EM, Auricchio A. Novel adeno-associated virus serotypes efficiently transduce murine photoreceptors. J. Virol. 2007; 81:11372–11380. [PubMed: 17699581]
14. Lebherz C, Maguire A, Tang W, Bennett J, Wilson JM. Novel AAV serotypes for improved ocular gene transfer. J. Gene Med. 2008; 10:375–382. [PubMed: 18278824]
15. Natkunarajah M, Trittibach P, McIntosh J, Duran Y, Barker SE, Smith AJ, Nathwani AC, Ali RR. Assessment of ocular transduction using single-stranded and self-complementary recombinant adeno-associated virus serotype 2/8. Gene Ther. 2008; 15:463–467. [PubMed: 18004402]
16. Maguire AM, High KA, Auricchio A, Wright JF, Pierce EA, Testa F, Mingozzi F, Bennicelli JL, Ying GS, Rossi S, Fulton A, Marshall KA, Banfi S, Chung DC, Morgan JI, Hauck B, Zelenaia O, Zhu X, Raffini L, Coppieters F, De Baere E, Shindler KS, Volpe NJ, Surace EM, Acerra C, Lyubarsky A, Redmond TM, Stone E, Sun J, McDonnell JW, Leroy BP, Simonelli F, Bennett J. Age-dependent effects of RPE65 gene therapy for Leber's congenital amaurosis: A phase 1 dose-escalation trial. Lancet. 2009; 374:1597–1605. [PubMed: 19854499]
17. Beltran WA, Boye SL, Boye SE, Chiodo VA, Lewin AS, Hauswirth WW, Aguirre GD. rAAV2/5 gene-targeting to rods: Dose-dependent efficiency and complications associated with different promoters. Gene Ther. 2010; 17:1162–1174. [PubMed: 20428215]
18. Stieger K, Colle MA, Dubreil L, Mendes-Madeira A, Weber M, Le Meur G, Deschamps JY, Provost N, Nivard D, Cherel Y, Moullier P, Rolling F. Subretinal delivery of recombinant AAV serotype 8 vector in dogs results in gene transfer to neurons in the brain. Mol. Ther. 2008; 16:916–923. [PubMed: 18388922]
19. Petersen-Jones SM, Bartoe JT, Fischer AJ, Scott M, Boye SL, Chiodo V, Hauswirth WW. AAV retinal transduction in a large animal model species: Comparison of a self-complementary AAV2/5 with a single-stranded AAV2/5 vector. Mol. Vis. 2009; 15:1835–1842. [PubMed: 19756181]
20. Bennett J, Maguire AM, Cideciyan AV, Schnell M, Glover E, Anand V, Aleman TS, Chirmule N, Gupta AR, Huang Y, Gao GP, Nyberg WC, Tazelaar J, Hughes J, Wilson JM, Jacobson SG. Stable transgene expression in rod photoreceptors after recombinant adeno-associated virus-mediated gene transfer to monkey retina. Proc. Natl. Acad. Sci. U.S.A. 1999; 96:9920–9925. [PubMed: 10449795]
21. Weber M, Rabinowitz J, Provost N, Conrath H, Folliot S, Briot D, Chérel Y, Chenuaud P, Samulski J, Moullier P, Rolling F. Recombinant adeno-associated virus serotype 4 mediates unique and exclusive long-term transduction of retinal pigmented epithelium in rat, dog, and nonhuman primate after subretinal delivery. Mol. Ther. 2003; 7:774–781. [PubMed: 12788651]
22. Bainbridge JW, Mistry A, Schlichtenbrede FC, Smith A, Broderick C, De Alwis M, Georgiadis A, Taylor PM, Squires M, Sethi C, Charteris D, Thrasher AJ, Sargan D, Ali RR. Stable rAAV-mediated transduction of rod and cone photoreceptors in the canine retina. Gene Ther. 2003; 10:1336–1344. [PubMed: 12883530]
23. Mancuso K, Hendrickson AE, Connor TB Jr. Mauck MC, Kinsella JJ, Hauswirth WW, Neitz J, Neitz M. Recombinant adeno-associated virus targets passenger gene expression to cones in primate retina. J. Opt. Soc. Am. A Opt. Image Sci. Vis. 2007; 24:1411–1416. [PubMed: 17429487]
24. Calcedo R, Vandenberghe LH, Gao G, Lin J, Wilson JM. Worldwide epidemiology of neutralizing antibodies to adeno-associated viruses. J. Infect. Dis. 2009; 199:381–390. [PubMed: 19133809]
25. Gao G, Vandenberghe LH, Wilson JM. New recombinant serotypes of AAV vectors. Curr. Gene Ther. 2005; 5:285–297. [PubMed: 15975006]
26. Vandenberghe LH, Wang L, Somanathan S, Zhi Y, Figueredo J, Calcedo R, Sanmiguel J, Desai RA, Chen CS, Johnston J, Grant RL, Gao G, Wilson JM. Heparin binding directs activation of T cells against adeno-associated virus serotype 2 capsid. Nat. Med. 2006; 12:967–971. [PubMed: 16845388]

27. Roy K, Stein L, Kaushal S. Ocular gene therapy: An evaluation of recombinant adeno-associated virus-mediated gene therapy interventions for the treatment of ocular disease. Hum. Gene Ther. 2010; 21:915–927. [PubMed: 20384478]

28. Grassi G, Maccaroni P, Meyer R, Kaiser H, D'Ambrosio E, Pascale E, Grassi M, Kuhn A, Di Nardo P, Kandolf R, Küpper JH. Inhibitors of DNA methylation and histone deacetylation activate cytomegalovirus promoter-controlled reporter gene expression in human glioblastoma cell line U87. Carcinogenesis. 2003; 24:1625–1635. [PubMed: 12869421]

29. Auricchio A, Kobinger G, Anand V, Hildinger M, O'Connor E, Maguire AM, Wilson JM, Bennett J. Exchange of surface proteins impacts on viral vector cellular specificity and transduction characteristics: The retina as a model. Hum. Mol. Genet. 2001; 10:3075–3081. [PubMed: 11751689]

30. Mancuso K, Hauswirth WW, Li Q, Connor TB, Kuchenbecker JA, Mauck MC, Neitz J, Neitz M. Gene therapy for red–green colour blindness in adult primates. Nature. 2009; 461:784–787. [PubMed: 19759534]

31. Lotery AJ, Yang GS, Mullins RF, Russell SR, Schmidt M, Stone EM, Lindbloom JD, Chiorini JA, Kotin RM, Davidson BL. Adeno-associated virus type 5: Transduction efficiency and cell-type specificity in the primate retina. Hum. Gene Ther. 2003; 14:1663–1671. [PubMed: 14633408]

32. Perry VH, Oehler R, Cowey A. Retinal ganglion cells that project to the dorsal lateral geniculate nucleus in the macaque monkey. Neuroscience. 1984; 12:1101–1123. [PubMed: 6483193]

33. Stein-Streilein J. Immune regulation and the eye. Trends Immunol. 2008; 29:548–554. [PubMed: 18838303]

34. Glatt H, Machemer R. Experimental subretinal hemorrhage in rabbits. Am. J. Ophthalmol. 1982; 94:762–773. [PubMed: 7180915]

35. Grossniklaus HE, Wilson DJ, Bressler SB, Bressler NM, Toth CA, Green WR, Miskala P. Clinicopathologic studies of eyes that were obtained postmortem from four patients who were enrolled in the submacular surgery trials: SST Report No. 16. Am. J. Ophthalmol. 2006; 141:93–104. [PubMed: 16386982]

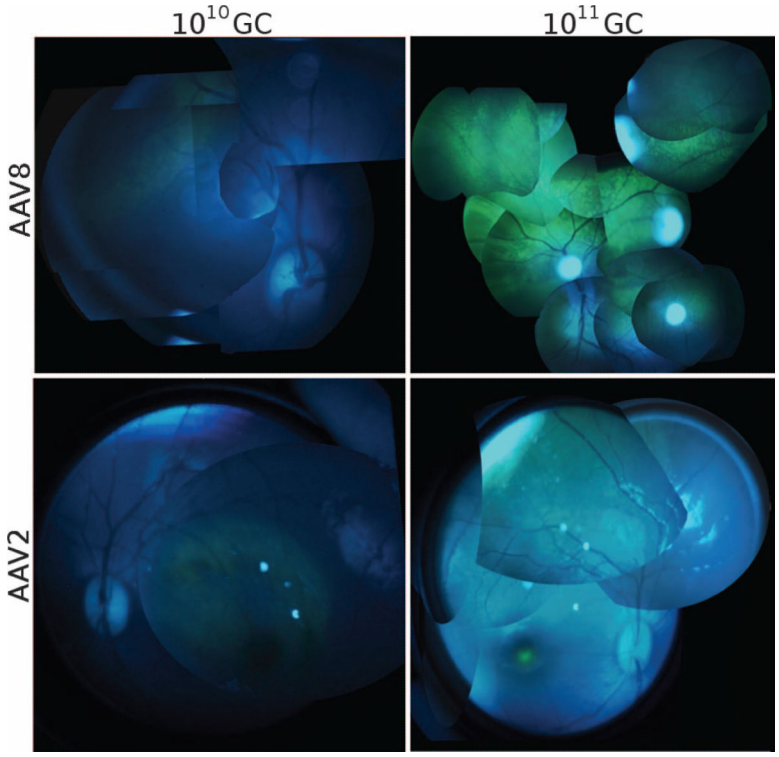

Fig. 1.

GFP expression in monkey retina. Montages of photographs taken in vivo of monkey retinas 1 month after subretinal injection of AAV2 or AAV8 at 10^{10} or 10^{11} genome copy (GC) doses. Blue light was used for GFP excitation; GFP expression, green areas. Clockwise from top left: animal 18204, right eye; 18155, left eye; 18221, right eye; 18226, left eye.

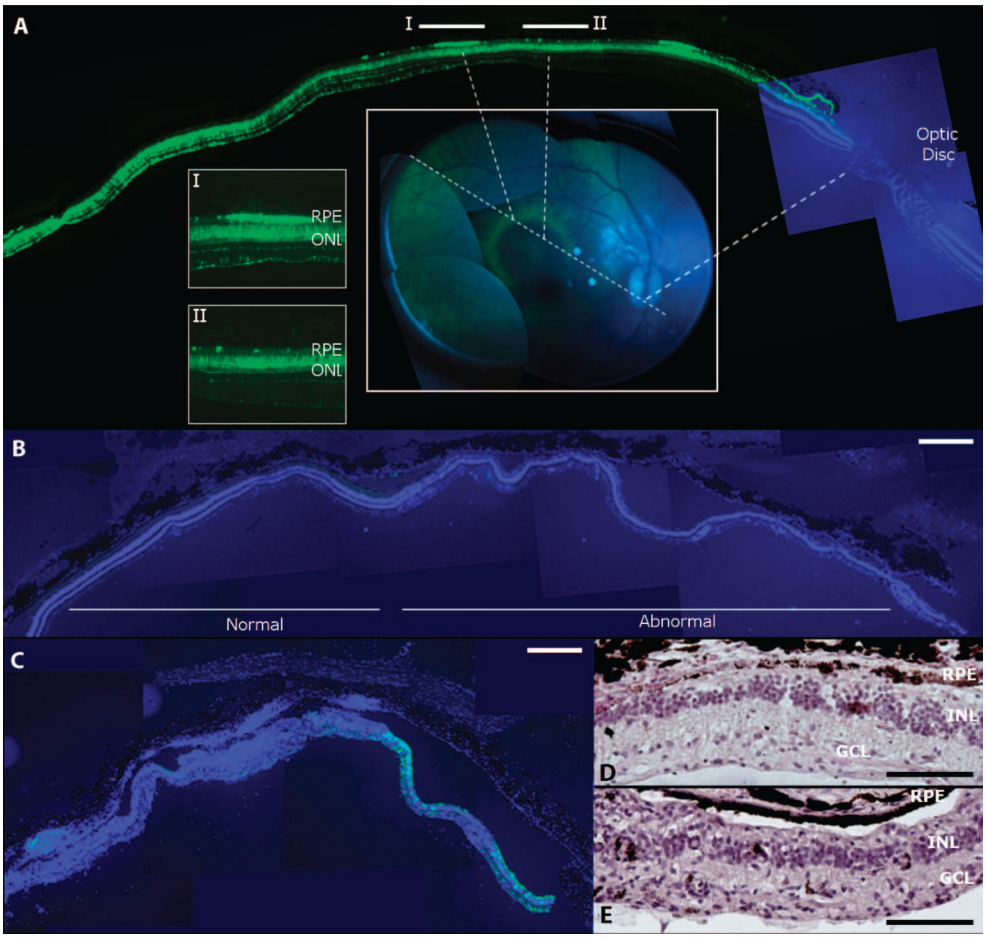

Fig. 2.

Retinal pathology after highest-dose vector injection in monkey retina. (**A**) Correlating histology and live retinal imaging identifies heterogeneous GFP expression in the vector-exposed part of the retina. A halo-like GFP pattern (green rim) was observed by imaging of the retina (center inset) after a 10^{11} genome copy dose injection of the AAV2 vector subretinally (animal 18226, right eye). Histology along an axis (center inset, dotted lines) that traverses the bleb, the optic disc, and the halo pattern (I and II) shows that the rims of the GFP halo (see inset I) are defined by GFP-positive RPE (green), whereas adjacent RPE does not express GFP (inset II) (GFP, green; DAPI staining of nuclei, blue). (**B**) DAPI staining (blue) of a section from a monkey eye injected subretinally with AAV2 (animal 18144, right eye) showing normal outer and inner nuclear layers with only minimal GFP fluorescence (green; left). This section is adjacent to a region where the nuclear layers are disturbed (abnormal; right). (**C**) Retina from the right eye of monkey 18199 after subretinal injection of AAV8 showing DAPI-stained nuclei (blue) and GFP expression (green) illustrates loss of retinal architecture and GFP on the left while retaining some GFP expression but abnormal retinal structure on the right. (**D**) Retinal section from animal 18144 (right eye) showing the abnormal portion in (B) stained with H&E. (**E**) H&E-stained section corresponding to the right part of the retina shown in (C) (animal 18199, right eye). Scale bars, 500 μm [(A) to (C)] and 100 μm [(D) and (E)].

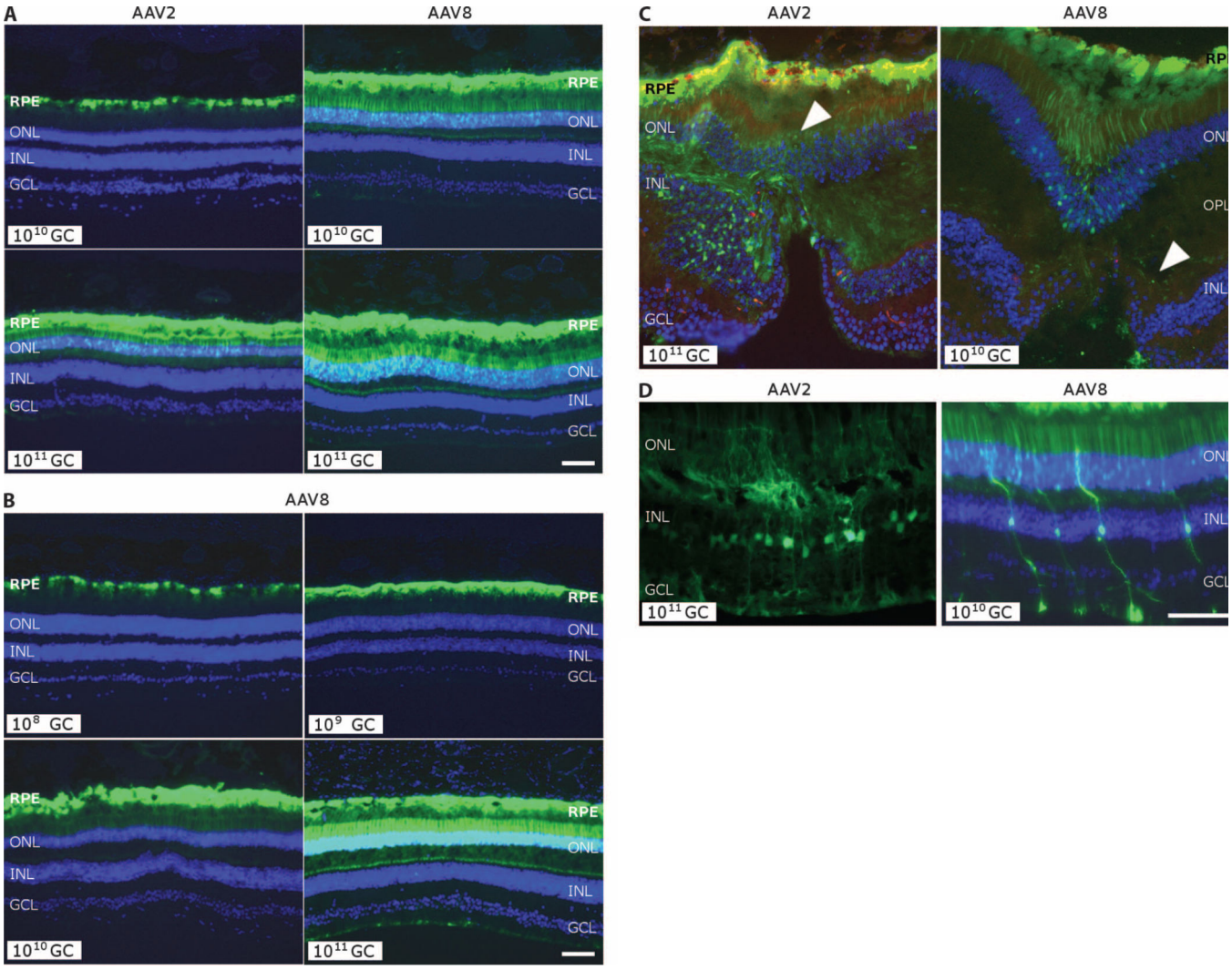

Fig. 3.

GFP transgene expression in the monkey retina. (**A**) Comparison of GFP expression from histological analysis of monkey retinas after subretinal injection with AAV2 or AAV8 with the designated number of genome copies. Clockwise from top left: animal 18168, left eye; animal 18238, right eye; animal 18155, right eye; animal 18226, right eye. (**B**) GFP expression after subretinal injection of AAV8 as a function of dose from 10^8 to 10^{11} genome copies (GC). Pictures are taken with equal exposure. Due to the intensity of GFP at the high dose, photoreceptor transduction in lower doses is less obvious. Clockwise from top left: animal 18204, left eye; animal 18217, left eye; animal 18208, right eye; animal 18238, right eye. (**C**) Cellular transduction characteristics after subretinal injection exposing the fovea to 10^{11} genome copies of AAV2 versus 10^{10} genome copies of AAV8. Both eyes show strong GFP expression in the RPE, but cone photoreceptors in the foveal pit of the AAV8-injected retina also are GFP-positive, as is the outer plexiform layer (OPL) in the AAV2-exposed retina (indicated by white arrowhead). (**D**) Transduction of Müller glial cells [with nuclei in the inner nuclear layer (INL)] after injection of AAV2 or AAV8. DAPI stain (blue) shows nuclear layers. Animal 18226, right eye (AAV2); animal 18204, right eye (AAV8). Scale

bars, 100 mm. RPE, retinal pigment epithelium; ONL, outer nuclear layer; GCL, ganglion cell layer.

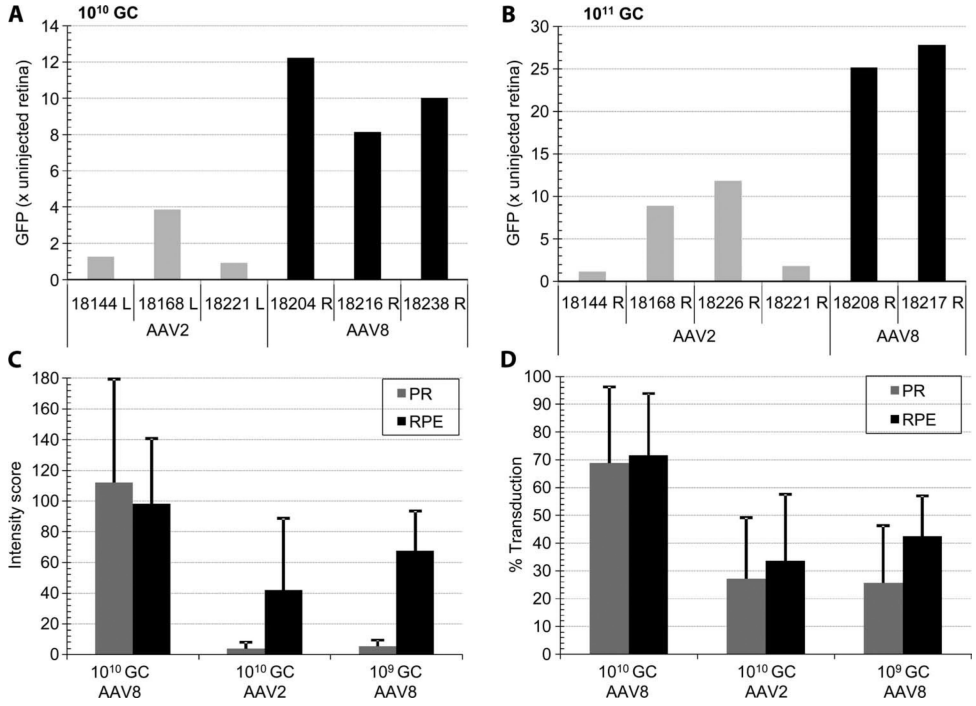

Fig. 4.

Quantitative analysis of retinal transduction with AAV2 and AAV8. (**A** and **B**) Whole-mount retinal fluorescence after necropsy. Eyeballs were fixed, and the cornea, lens, and vitreous humor were removed to expose the posterior eye cup. Relative fluorescence was measured in a Xenogen Lumina IVIS imager and normalized to the fluorescence signal from an uninjected control eye. Eyes injected with 150 μl of 10^{10} genome copies (A) and 10^{11} genome copies (B) of AAV2 or AAV8 vector are shown. (**C** and **D**) Morphometric analysis of RPE and photoreceptor (PR) transduction by AAV2 and AAV8. Relative intensity (C) and relative area (D) of the GFP expression signal in RPE and PR were established at doses of 10^9 and 10^{10} genome copies based on morphometric histological analysis within the vector-exposed area. Numbers shown identify the animal used. L, left eye; R, right eye.

Table 1

Experimental design and surgical and ophthalmoscopic findings. GFP expression intensities graded ophthalmoscopically correlate with AAV2 and AAV8 dose. Injection of AAV8 results in greater GFP expression than injection of AAV2 dose per dose. Gray shaded areas indicate exclusion from quantitative postmortem analysis because of injection anomalies or complications, including leakage into the vitreous humor (cf. notes). Percent of subretinal (SR) and intravitreal (IV) spaces reflect estimates of vector deposits in these areas. GFP expression scores range from 0 (no visible expression) to 4 (broad, intense staining). They reflect a subjective composite of both intensity and area of transduction as observed by indirect ophthalmoscopy. F, foveal; V, 135-µl volume injected instead of 150 µl; B, blood (intraretinal or subretinal); ID, animal identification number; IR, intraretinal; I, injector defect required a second successful retinal application; GFP, green fluorescent protein; GC, genome copies.

					Right							Left						
									GFP score							GFP score		
	Animal ID	Weight (kg)	Sex	Duration (days)	Dose (10^x GC)	SR (%)	IV (%)	Notes	1 week	1 month	4 months	Dose (10^x GC)	SR (%)	IV (%)	Notes	1 week	1 month	4 months
AAV8	18216	5.60	♂	155	10	100	0	F	0	4	4	8	100	0		0	0	1
	18173	3.80	♀	153		15	85		0	3.5	3		100	0		0	0	3
	18204	5.60	♂	153		100	0	F	2	4	3		100	0		0.5	0	2
	18234	4.35	♂	155		90	10	V	0	3.5	4		100	0	B (IR)	0	0.5	0
	18238	3.50	♂	155		100			1	4	4		100	0		0	0	0
	18217	4.85	♂	162	11	100	0		0	4F	4F	9	87	13		0	2	2
	18155	3.50	♀	160		87	13		0.5	4F	4		100	0		0	2	3
	18180	3.25	♀	160		40	60	B (SR)	0	4F	4F		100	0		0	2	2
	18199	5.80	♂	162		100	0	I	0.5	4F	4F		100	0		0	2	4
	18208	5.20	♂	162		100	0	B (SR)	0	4F	4F		100	0		0	2	2
AAV2	18144	4.50	♀	139	11	100	0		0	4	4F	10	100	0		0	3	0
	18168	2.80	♀	139		100	0		0	3	4		100	0		0	2	4
	18226	5.75	♂	140		100	0	B (SR); F	0	3F	4F		13	87	F	0	4	2F
	18221	4.85	♂	140		100	0	F	0	1	3		100	0		0	1	0

Table 2

Host immune responses and toxicology. Neutralizing antibodies (NABs) directed at the AAV capsid trend upward with higher dosing in both intraocular fluid and serum. A T cell response (detected by ELISPOT assay) directed at GFP developed in two animals exposed to the highest dose of either AAV2 or AAV8. Histopathological analyses showed retinal infiltrates (observed in H&E-stained sections) in the retinas of those animals as well as in the retina of one animal that had experienced a retinal hemorrhage during the injection procedure (“hemorrhage”). Analyses of NAB responses compared baseline levels of anterior chamber (AC) fluid and serum with samples at the termination of the experiment. The T cell–mediated immune response to GFP compared baseline measurements (“Pre-ex. capsid T”) with measurements taken 2 weeks after injection of AAV (“Capsid T 2w”) and at the termination of the study at 20 weeks (“GFP T 20w”). There was no correlation between expression of GFP in the optic nerve or optic chiasm and an immune response. Animals are identified by number. L, left eye; R, right eye; GFP, green fluorescent protein.

Vector serotype	**AAV8**										**AAV2**			
Dose	**10^8 genome copies**					**10^9 genome copies**					**10^{10} genome copies**			
ID	**18238L**	**18234L**	**18173L**	**18216L**	**18204L**	**18199L**	**18155L**	**18217L**	**18208L**	**18180L**	**18144L**	**18168L**	**18221L**	**18226L**
Retinal degeneration	−	−	−	−	−	−	−	−	−	−	+	−		−
Retina infiltrates	−	−	−	−	−	−	−	−	−	−	+	−	−	−
Optic nerve GFP	−	−	−	−	−	−	−	−	−	−	−	−	−	−
AC NAB	<1:20	<1:20	<1:20	<1:20	<1:20	<1:20	<1:20	<1:20	<1:20	<1:20	<1:20	1:20	<1:20	<1:20
Hemorrhage			+											+
Dose	**10^{10} genome copies**					**10^{11} genome copies**					**10^{11} genome copies**			
ID	**18238R**	**18234R**	**18173R**	**18216R**	**18204R**	**18199R**	**18155R**	**18217R**	**18208R**	**18180R**	**18144R**	**18168R**	**18221R**	**18226R**
Retinal degeneration	−	−	−	−	−	+	−	−	+	−	+	−		−
Retina infiltrates	−	−	−	−	−	+	−	−	+	−	+	−	−	−
Optic nerve GFP	+	−	−	−	−	+	+	+	+	+	+	+	+	+
AC NAB	<1:20	<1:20	<1:20	<1:20	<1:20	<1:20	1:160	<1:20	1:80	<1:20	1:80	1:20	<1:20	1:40
Hemorrhage									+	+				
Chiasm GFP	−	−	−	−	−	+	+	+	+	+	+	+	+	+
Pre-ex. capsid T	+	+	+	+	−	−	+	+	+	−	−	−	+	+
Capsid T 2w	−	−	−	−	−	−	−	−	−		−	−	−	−
GFP T 20w	−	−	−	−	−	+	−	−	−	−	+	−	−	−
Serum NAB	<1:20	<1:20	1:80	<1:20	1:80	<1:20	1:320	1:160	1:80	1:80	1:640	1:160	<1:20	1:320